

April 6, 2019

Implications of Cosmic Microwave Background Anisotropies for Large Scale Variations in Hubble's Constant

Yun Wang, David N. Spergel, and Edwin L. Turner

*Princeton University Observatory**Peyton Hall, Princeton, NJ 08544**email: ywang,dns,elt@astro.princeton.edu*

Abstract

Low amplitude (linear regime) cosmic density fluctuations lead to spatial variations in the locally measurable value of H_0 (denoted as H_L), $\delta_H \equiv (H_L - H_0)/H_0$, which are of order 3 – 6% (95% confidence interval) in a sphere of $200 h^{-1}\text{Mpc}$ in diameter, and of order 1 – 2% in a sphere of $400 h^{-1}\text{Mpc}$ in diameter, for three currently viable structure formation models (tilted CDM, ΛCDM , and open CDM) as normalized by the 4 year COBE DMR data.

However, the true matter distribution power spectrum may differ from any of the currently viable models. For example, it may contain sharp features which have escaped detection so far. The measured CMB dipole velocity (the Galaxy's peculiar velocity with respect to the CMB rest frame) provides additional constraints on the probability distribution of δ_H that supplement our limited knowledge of the power spectrum. For a matter power spectrum which consists of the smooth power spectrum of a viable cosmological model plus a delta-function bump, we find that given the CMB dipole velocity, the 95% CL upper limit of $|\delta_H|$ increases approximately by a factor of two, but the

probability distribution of δ_H is non-Gaussian, with increased probability at small δ_H compared to Gaussian. Abandoning model power spectra entirely, we find that the observed CMB dipole velocity alone provides a very robust limit, $\sqrt{\langle \delta_H^2 \rangle_R} < 10.5 h^{-1} \text{Mpc}/R$ at 95% CL, in a sphere of radius R , for an arbitrary power spectrum.

Thus, variations between currently available local measures of H_0 and its true global value of a few to several percent are to be expected and differences as large as 10% are possible based on our current knowledge of the CMB anisotropies.

1. Introduction

In the standard gravitational instability scenario (Peebles 1980, Peebles 1993) for cosmic structure formation, linear growth of density fluctuations is produced by, and produces, spatial variations of the expansion rate. In this rather generic scenario, such variations are the inevitable implication of the extremely large scale structures which have been detected in the galaxy distribution, primarily via redshift surveys (e.g., DaCosta et al. 1994, Lauer & Postman 1994, Lin et. al. 1996, Tadros & Efstathiou 1996).

The connection of such expansion rate variations, which are often thought of as peculiar velocity fields, to the large scale density distribution is of direct interest (Strauss & Willick 1995) but is also potentially important as a source of systematic error in attempts to measure Hubble’s constant H_0 , the overall mean expansion rate of the Universe. In particular, if the expansion rate is correctly measured in a local volume which is not sufficiently large compared to the biggest significant cosmic structures, the strong possibility of a difference between it and the true cosmic value of H_0 must be considered.

This potential problem has long been known in principle, was emphasized in the context of modern structure formation models by Turner, Ostriker, & Cen (1992) and has subsequently been considered by several authors (Wu et al. 1995, Nakamura et al. 1995, Nakao et al. 1995, Shi, Widrow, & Dursi 1996, Wu et al. 1996, Shi & Turner 1997). The issue is of greater interest than ever at present for two reasons: First, measurements of H_0 by conventional distance ladder techniques have improved dramatically and now achieve credible precisions of order 10 to 20 percent. It follows that a systematic difference between local and global expansion rates of a comparable fractional size are important sources of error. Second, there is suggestive, though not yet compelling, evidence that direct physical methods for measuring H_0 on extremely large scales (out to redshifts of order unity) (Birkinshaw, Hughes, & Arnaud 1991, Jones et al. 1993, Schechter et al. 1997, Kundic et

al. 1997) give a somewhat smaller value than the best distance ladder determinations which apply out to redshifts of a tenth or less (Graham et al. 1997, Tonry et al. 1997, Eastman, Schmidt & Kirshner 1996).

In this paper we attempt to exploit our best and most direct empirical information about large scale (linear) cosmic density fluctuations, namely observed anisotropies in the cosmic microwave background (CMB), in order to predict and/or constrain the expected resulting variations in the expansion rate. Specifically, we study these intrinsic fluctuations, $\delta_H \equiv (H_L - H_0)/H_0$, where H_L is the local measure of H_0 , in terms of the matter distribution power spectrum $P(k)$.

In fact, we present here three separate calculations of this sort, proceeding from the one which gives the strongest result but which is most model dependent to the one which is weakest but most robust (model independent). First, we simply base our input $P(k)$ on standard structure formation models in terms of its shape and use CMB observations only to set the overall normalization or amplitude. Here, our results agree with recent work by Shi & Turner (1997). Second, we consider an input $P(k)$ with a shape and amplitude constrained by CMB fluctuations; for some scales (k values) $P(k)$ is effectively directly observed, but we allow for the possibility of strong features on those scales not directly sampled by currently available data by imposing limits based on the CMB dipole (the Galaxy’s peculiar velocity with respect to the CMB rest frame). Third, we impose no constraints at all on the input $P(k)$ (which does not even appear explicitly in this calculation) other than that it be Gaussian and not violate the aforesaid CMB dipole constraint.

Section 2 contains general expressions for δ_H and related variables. In Section 3, we compute δ_H for matter power spectra given by three viable cosmological models which are normalized by the 4 year COBE DMR data and satisfy constraints from large scale

structure data. In Section 4, we study the effects of unexpected features in $P(k)$ which may boost δ_H by adding a delta-function bump to a smooth matter power spectrum given by a viable cosmological model. In Section 5, we apply Bayesian statistics to derive robust upper limits on δ_H and related variables, using the CMB dipole velocity of $v=627$ km/s (Kogut et al. 1993, Fixsen et al. 1994); these upper limits are independent of the actual form of the matter power spectrum. Section 6 contains discussions and a summary.

2. General Expressions

For an observer at \mathbf{r}_i who measures the Hubble’s constant by summing over the radial recession velocity divided by distance of N objects located at \mathbf{r}_j , ($j = 1, 2, \dots, N$) (Turner, Ostriker, & Cen 1992)

$$\delta_H(\mathbf{r}_i) \equiv \frac{H(\mathbf{r}_i) - H_0}{H_0} = \frac{1}{N} \sum_{j \neq i} \frac{\mathbf{v}_j \cdot (\mathbf{r}_j - \mathbf{r}_i)}{H_0 |\mathbf{r}_j - \mathbf{r}_i|^2}. \quad (1)$$

To find δ_H for a sphere of radius R centered around \mathbf{x} , we write (Shi, Widrow, & Dursi 1996)

$$\delta_H(\mathbf{x})^R = \int d^3\mathbf{y} \frac{\mathbf{v}(\mathbf{y})}{H_0} \cdot \frac{\mathbf{y} - \mathbf{x}}{|\mathbf{y} - \mathbf{x}|^2} W(\mathbf{y} - \mathbf{x}), \quad (2)$$

where $W(\mathbf{y} - \mathbf{x})$ is the top hat window function with radius R ,

$$W(\mathbf{y} - \mathbf{x}) = \begin{cases} (4\pi R^3/3)^{-1}, & |\mathbf{y} - \mathbf{x}| \leq R \\ 0, & |\mathbf{y} - \mathbf{x}| > R \end{cases} \quad (3)$$

In linear perturbation theory (Peebles 1993, 1980), the Fourier component of $\mathbf{v}(\mathbf{y}) = (2\pi)^{-3} \int d^3\mathbf{k} \mathbf{v}_k \exp(-i\mathbf{k} \cdot \mathbf{y})$ is

$$\mathbf{v}_k = \frac{\Omega_0^{0.60} H_0}{ik} \delta_k \hat{k}, \quad (4)$$

for an open or flat universe. δ_k is the Fourier component of the density fluctuation. Hence

$$\delta_H(\mathbf{x})^R = \frac{\Omega_0^{0.60}}{(2\pi)^3} \int d^3\mathbf{k} \delta_k \mathcal{L}(kR) e^{-i\mathbf{k} \cdot \mathbf{x}}, \quad (5)$$

where

$$\mathcal{L}(x) = \frac{3}{x^3} \left(\sin x - \int_0^x dy \frac{\sin y}{y} \right). \quad (6)$$

Note that $\mathcal{L}(x \rightarrow 0) = -1/3$, and $\mathcal{L}(x) < 0$, as expected; overdensities ($\delta_k > 0$) lead to infall, which leads to the underestimate of the Hubble's constant ($\delta_H < 0$).

δ_H is a Gaussian random variable, with mean 0 and variance

$$\langle \delta_H^2 \rangle_R = \frac{\Omega_0^{1.20}}{2\pi^2 R^2} \int_0^\infty dk P(k) [(kR)\mathcal{L}(kR)]^2. \quad (7)$$

The power spectrum $P(k) = |\delta_k|^2$. The variance of density fluctuations in a sphere of radius R is

$$\left\langle \left(\frac{\delta\rho}{\rho} \right)^2 \right\rangle_R = \frac{1}{2\pi^2 R^2} \int_0^\infty dk P(k) \left\{ (kR) \left[\frac{3j_1(kR)}{kR} \right] \right\}^2. \quad (8)$$

Clearly, the fluctuations in the measured expansion rate stem directly from the fluctuations in matter density.

We can define $\Omega_L \equiv 8\pi G\rho_L/(3H_L^2)$. To lowest order in $\delta\rho/\rho$ and δ_H , $\delta_\Omega \equiv (\Omega_L - \Omega_0)/\Omega_0 = \delta\rho/\rho - 2\delta_H$. We find

$$\langle \delta_\Omega^2 \rangle_R = \frac{1}{2\pi^2 R^2} \int_0^\infty dk P(k) \left\{ (kR) \left[\frac{3j_1(kR)}{kR} - 2\Omega_0^{0.60} \mathcal{L}(kR) \right] \right\}^2. \quad (9)$$

Note that the fluctuations in Ω_L are contributed additively by $\delta\rho/\rho$ and δ_H ($\mathcal{L}(x) < 0$).

$\Omega_L = 8\pi G\rho_L/(3H_L^2)$ is related but not identical to the locally measured Ω (by counting matter or dynamical methods).

The variance of peculiar velocity \mathbf{v} and bulk flow velocity \mathbf{v}_R (variance of peculiar velocity in a sphere of radius R) also depend on $P(k)$,

$$\begin{aligned} \langle \mathbf{v}^2 \rangle &= \frac{\Omega_0^{1.20} H_0^2}{2\pi^2} \int_0^\infty dk P(k), \\ \langle \mathbf{v}^2 \rangle_R &= \frac{\Omega_0^{1.20} H_0^2}{2\pi^2} \int_0^\infty dk P(k) \left[\frac{3j_1(kR)}{kR} \right]^2. \end{aligned} \quad (10)$$

Note that $\langle \delta_H^2 \rangle_R$, $\langle (\delta\rho/\rho)^2 \rangle_R$, $\langle \delta_\Omega^2 \rangle_R$, and $\langle \mathbf{v}^2 \rangle_R$ are all proportional to integrals over $P(k)$ multiplied by a window function $W(kR)$; Fig.1 shows these window functions. Note that the window function of $\langle \delta_H^2 \rangle_R$ is somewhat similar to that of $\langle (\delta\rho/\rho)^2 \rangle_R$ and $\langle \delta_\Omega^2 \rangle_R$, but very different from that of $\langle \mathbf{v}_R^2 \rangle$. Also, $\langle \delta_H^2 \rangle_R$, $\langle (\delta\rho/\rho)^2 \rangle_R$, and $\langle \delta_\Omega^2 \rangle_R$ all decrease much faster with R (the radius of the observed volume) than $\langle \mathbf{v}_R^2 \rangle$ (note that we have factored $1/R^2$ out of the integrals for $\langle \delta_H^2 \rangle_R$, $\langle (\delta\rho/\rho)^2 \rangle_R$, and $\langle \delta_\Omega^2 \rangle_R$), while $\langle \mathbf{v}^2 \rangle$ is independent of the size of the observed volume.

Even though δ_H is caused by the presence of non-zero peculiar velocities [see Eq.(1)], it has only weak correlations with the measures of the peculiar velocity field.

3. Theoretical Power Spectra with CMB Normalization

Let us consider cosmological structure formation models which simultaneously satisfy constraints from the observed LCRS power spectrum (Lin et. al. 1996), the Hubble's constant range of $0.5 \lesssim h \lesssim 0.8$, cluster abundance results, and the reasonable assumption that LCRS galaxies are approximately unbiased on large scales relative to the mass normalization provided by the 4 year COBE DMR data. Following Lin et. al. 1996, we assume that in the linear regime

$$P_{galaxy, redshift\ space}(k) \simeq b^2 \left(1 + \frac{2}{3} \frac{\Omega_0^{4/7}}{b} + \frac{1}{5} \frac{\Omega_0^{8/7}}{b^2} \right) P_{mass, real\ space, linear}(k). \quad (11)$$

Three viable models are: (1) TCDM: $\Omega_0 = 1$, $n = 0.7$, $h = 0.5$, $\Omega_b = 0.05$, $b = 1.3$; (2) Λ CDM: $\Omega_0 = 0.5 = \Omega_\Lambda$, $n = 1$, $h = 0.5$, $\Omega_b h^2 = 0.015$, $b = 0.9$; (3) OCDM: $\Omega_0 = 0.5$, $n = 1$, $h = 0.65$, $\Omega_b h^2 = 0.015$, $b = 0.9$.

The power spectrum of a model is given by

$$\frac{P(k)}{h^{-3} \text{Mpc}^3} = P_0 \left(\frac{k}{\text{Mpc}^{-1} h} \right)^n T^2(q), \quad (12)$$

where $P_0 \equiv 2\pi^2 (10^5 \delta_{hor} \cdot 90)^2 \cdot 3000^{n-1}$. The 4 year COBE DMR data give (Bunn & White 1997)

$$10^5 \delta_{hor} = \begin{cases} 1.94 \Omega_0^{-0.785-0.05 \ln \Omega_0} \exp[-0.95 (n-1) - 0.169 (n-1)^2], & \Omega = 1; \\ 1.95 \Omega_0^{-0.35-0.19 \ln \Omega_0}, & \Omega < 1, n = 1. \end{cases} \quad (13)$$

$T(q)$ is the CDM transfer function, given by (Bardeen et. al. 1986)

$$T(q) = \frac{\ln(1 + 2.34 q)}{2.34 q} \left[1 + 3.89 q + (16.1 q)^2 + (5.46 q)^3 + (6.71 q)^4 \right]^{-1/4}, \quad (14)$$

where $q = k/(h\Gamma)$, Γ is the shape parameter. We use (Hu & Sugiyama 1996)

$$\Gamma = \Omega_0 h \alpha^{1/2} \Theta_{2.7}^{-2}, \quad (15)$$

where $\Theta_{2.7} = 2.726 K / 2.7 K$, and

$$\begin{aligned} \alpha &= a_1^{-\Omega_b/\Omega_0} a_2^{-(\Omega_b/\Omega_0)^3}, \\ a_1 &= (46.9 \Omega_0 h^2)^{0.670} \left[1 + (32.1 \Omega_0 h^2)^{-0.532} \right], \\ a_2 &= (12.0 \Omega_0 h^2)^{0.424} \left[1 + (45.0 \Omega_0 h^2)^{-0.582} \right]. \end{aligned} \quad (16)$$

For the three models considered, $\Gamma = 0.467$ (TCDM), 0.223 (Λ CDM), and 0.299 (OCDM) respectively.

Figs.2-5 show $\langle \delta_H^2 \rangle_R$, $\langle (\delta\rho/\rho)^2 \rangle_R$, $\langle \delta_\Omega^2 \rangle_R$, and $\langle \mathbf{v}^2 \rangle_R$, as functions of R , for the three models (TCDM, Λ CDM, and OCDM). Figure 2 indicates, for example, that a *perfect* measurement of the local expansion rate in a sphere of diameter 20,000 km/s ($200 h^{-1}$ Mpc) would provide a 95 percent confidence interval determination of the global value of H_0 with a width of 3 to 6 percent, depending on the adopted structure formation model.

4. Smooth Power Spectra with a Feature on Unobserved Scales

The COBE observations of CMB fluctuations on scales larger than 7° (Bennett et al. 1996) directly probe the potential fluctuations on scales larger than $300 h^{-1}$ Mpc. It

is possible to smoothly connect the COBE measurements to observations of large scale structure. In fact, there is a family of cold dark matter models (tilted CDM, open CDM, Lambda-dominated CDM, mixed dark matter) that are consistent with both measurements of large-scale structure on scales of $\sim 1 - 60$ Mpc and CMB observations on large scales (Ratra et al. 1997, Bunn & White 1997).

There are, however, a number of observations that suggest that the amplitude of fluctuations on the $60 - 300 h^{-1}$ Mpc scale exceeds that predicted by CDM models or by smooth interpolations between the scales probed by galaxy surveys and the COBE observations: Lauer & Postman (1994) measure much larger bulk flows than predicted by standard cosmological models (Strauss et al. 1995); deep pencil beam surveys detect excess power on scale of $\sim 100/h$ Mpc (Broadhurst et al. 1990, Cohen et al. 1996); two-dimensional measures of the power spectrum in the Las Campanas redshift survey also find excess power on the $100/h$ Mpc scale (Landy et al. 1996); and K-band galaxy counts can be interpreted as indicating a very large scale local underdensity region (Phillips & Turner 1998). If the ratio of the baryon density to the closure density, $\Omega_b h^2$, is close to the low value suggested by the D/H measurements of Songaila, Wampler & Cowie (1997), then recent CMB measurements on the 1-2 degree scale (Netterfield et al. 1997) would also imply excess power near the $100/h$ Mpc scale. Even if $\Omega_b h^2$ is large, it is difficult to use CMB observations to place an upper limit on density fluctuations on this scale as CMB fluctuations on scales smaller than that probed by COBE may have been suppressed by reionization of the intergalactic medium at $z > 20$.

These observations suggest that $P(k)$ is not smooth, but may have some feature on the $60 - 300 h^{-1}$ Mpc scale. There are several interesting physical processes acting on these scales because of the horizon size at the matter-radiation transition and at baryon-photon decoupling, so it is quite possible that there is new physics acting on these scales. Since

we are trying to constrain the uncertainties in the Hubble's constant due to large scale structure, we will study the possibility of excess power by adding a delta-function bump to a smooth matter power spectrum $P_0(k)$ given by a viable cosmological model. Let us write

$$P(k) = P_0(k) + A\delta(k - k_0), \quad (17)$$

We take $P_0(k)$ given by the tilted CDM model (TCDM) as a convenient smooth functional form, with $n = 0.7$, $\Omega_0=1$, $\Omega_b = 0.05$, and $h = 0.5$. Since $\int_0^\infty dk P_0(k) = 828.808 h^{-2}\text{Mpc}^2$, and $\tilde{A} = \Omega_0^{1.20} H_0^2 / (2\pi^2) [\int_0^\infty dk P_0(k) + A]$ is less than $(1831 \text{ km/s})^2$ at 95% CL (see the following section for more details), we find that $A/(2\pi^2) \leq 293.3 h^{-2}\text{Mpc}^2$ at 95% CL. Calculations show that the delta function spike has the most significant effect on the bulk flow velocity $\sqrt{\langle \mathbf{v}^2 \rangle}_R$.

Now we compute the probability distribution of δ_H measured in a sphere of radius R , given the CMB dipole velocity of $v=627 \text{ km/s}$. Using the Bayesian theorem, we find

$$P(\delta_H|v)_R = \sum_{\tilde{A}} P(\delta_H|\tilde{A})_R P(\tilde{A}|v) \propto \sum_{\tilde{A}} P(\delta_H|\tilde{A})_R P(v|\tilde{A}) P(\tilde{A}), \quad (18)$$

where

$$P(\delta_H|\tilde{A})_R = \frac{1}{\sqrt{2\pi\langle\delta_H^2\rangle_R}} \exp\left(-\frac{\delta_H^2(R)}{2\langle\delta_H^2\rangle_R}\right). \quad (19)$$

$\langle\delta_H^2\rangle_R$ is a complicated function of \tilde{A} . For the power spectrum of Eq.(17), we have

$$\begin{aligned} \langle \mathbf{v}^2 \rangle &= \tilde{A} = \alpha_1 + \alpha_2 A, \\ \langle \delta_H^2 \rangle_R &= \beta_1(R) + \beta_2(R, k_0) A. \end{aligned} \quad (20)$$

We have defined

$$\begin{aligned} \alpha_1 &\equiv \frac{\Omega_0^{1.20} H_0^2}{2\pi^2} \int_0^\infty dk P_0(k), & \alpha_2 &\equiv \frac{\Omega_0^{1.20} H_0^2}{2\pi^2}, \\ \beta_1 &\equiv \frac{\Omega_0^{1.20}}{2\pi^2 R^2} \int_0^\infty dk P_0(k) [(kR)\mathcal{L}(kR)]^2, \\ \beta_2 &\equiv \frac{\Omega_0^{1.20}}{2\pi^2 R^2} [(k_0 R)\mathcal{L}(k_0 R)]^2. \end{aligned} \quad (21)$$

The parameter A characterizes the departure of the power spectrum from the underlying smooth power spectrum; we expect the probability of A to decrease with increasing A . Let us use the prior probability

$$P(A) = \begin{cases} 1/A, & A \geq A_c; \\ 0, & A < A_c. \end{cases} \quad (22)$$

A_c is a cut-off motivated by physical considerations. We consider two choices for the cut-off A_c :

- (1) $A_c = \alpha_1/\alpha_2 = \int_0^\infty dk P_0(k)$;
- (2) $A_c = 0.1 \alpha_1/\alpha_2 = 0.1 \int_0^\infty dk P_0(k)$.

The first choice of A_c indicates the reasonable upper limit of A_c , while the second choice indicates a typical value of A_c of interest.

The probability distribution of δ_H given the value of v is

$$P(\delta_H|v)_R = \frac{1}{\mathcal{N}\sqrt{2\pi\beta_1}} \int_0^{x_c} dx \frac{x}{(x+1)^{3/2}(x+x_1)^{1/2}} \exp \left\{ - \left[\frac{3v^2 x}{2\alpha_1(x+1)} + \frac{\delta_H^2 x}{2\beta_1(x+x_1)} \right] \right\}. \quad (23)$$

where

$$x_c \equiv \frac{\alpha_1}{\alpha_2} \frac{1}{A_c}, \quad x_1 \equiv \frac{\alpha_1\beta_2}{\alpha_2\beta_1}, \quad (24)$$

and

$$\mathcal{N} \equiv \int_0^{x_c} dx \frac{x^{1/2}}{(x+1)^{3/2}} \exp \left\{ - \frac{3v^2 x}{2\alpha_1(x+1)} \right\} \quad (25)$$

The variance of δ_H given $v = 627$ km/s is

$$\langle \delta_H^2 | v \rangle_R = \frac{\beta_1}{\mathcal{N}} \int_0^{x_c} dx \frac{x+x_1}{x^{1/2}(x+1)^{3/2}} \exp \left\{ - \frac{3v^2 x}{2\alpha_1(x+1)} \right\}. \quad (26)$$

Figs.6-8 show $P(\delta_H|v)_R$ for $k_0 = 0.01 h \text{ Mpc}^{-1}$ and $R = 40, 100, 500 h^{-1} \text{ Mpc}$ respectively. The solid and dashed lines are the distributions given by Eq.(23), with $x_c = 10$

($A_c = 0.1 \alpha_1/\alpha_2$) and $x_c = 1$ ($A_c = \alpha_1/\alpha_2$) respectively; the dotted lines are Gaussian distributions with the same variance [given by Eq.(26)] for $x_c = 10$. Note that $P(\delta_H|v)_R$ becomes increasingly non-Gaussian for increasing R . Table 1 lists the 95% CL upper limits on $|\delta_H|$, δ_H^0 , as well as $2\sigma \equiv 2\sqrt{\langle\delta_H^2|v\rangle_R}$, the 95% CL upper limit on δ_H if its distribution were Gaussian.

	R	40Mpc h^{-1}	100Mpc h^{-1}	500Mpc h^{-1}
$x_c = 10$	δ_H^0	0.115	5.50×10^{-2}	9.44×10^{-3}
	2σ	0.120	6.13×10^{-2}	1.05×10^{-2}
$x_c = 1$	δ_H^0	0.135	8.67×10^{-2}	1.59×10^{-2}
	2σ	0.143	9.56×10^{-2}	1.75×10^{-2}

It is not surprising that our results depend on the prior probability $P(A)$ via the cut-off A_c , since different choices of A_c represent different input of physical information. It is worth noting that the 95% CL upper limit on $|\delta_H|$ is close to 10% for $R \geq 100 \text{ Mpc } h^{-1}$ with the largest reasonable A_c (when the contribution to the mean square peculiar velocity by the bump in $P(k)$ is greater or equal to the contribution by the underlying smooth power spectrum).

Also note that in our Bayesian statistics, the measured CMB dipole velocity of $v = 627 \text{ km/s}$ has the effect of distorting the distribution of δ_H away from Gaussian by increasing the probability of smaller δ_H .

5. A Robust Upper Limit on the Variance of δ_H

The CMB dipole velocity of $v \equiv |\mathbf{v}|=627 \text{ km/s}$ is the Galaxy’s peculiar velocity with respect to the CMB rest frame. In the previous section, it provided us with a constraint on

possible unobserved features in $P(k)$, but we can in fact use it in a more fundamental way to provide a single integral constraint on $P(k)$ which is related in a simple way to possible expansion rate variations, as described below. We can infer the distribution of $\tilde{A} \equiv \langle \mathbf{v}^2 \rangle$ by using the Bayesian theorem,

$$P(\tilde{A}|v) = \frac{P(v|\tilde{A})P(\tilde{A})}{P(v)} \propto P(v|\tilde{A})P(\tilde{A}). \quad (27)$$

$P(\tilde{A})$ is the prior probability of \tilde{A} . Since $\tilde{A}/3$ is the variance of the Gaussian variable v_x (x component of \mathbf{v}), it is most reasonable to choose $P(\tilde{A}) = 1/\tilde{A}$. For diagnostic on the dependence on the prior, let us write

$$P(\tilde{A}) = \begin{cases} 1/\tilde{A}, & \tilde{A} \geq \tilde{A}_c; \\ 0, & \tilde{A} < \tilde{A}_c. \end{cases} \quad (28)$$

$\tilde{A}^{1/2} < \tilde{A}_0^{1/2}$ at 95% CL, with $\tilde{A}_0^{1/2}$ given by

$$\int_0^{\tilde{A}_0} P(\tilde{A}|v) d\tilde{A} = 0.95. \quad (29)$$

Using

$$P(v|\tilde{A}) \propto \frac{v^2}{\tilde{A}^{3/2}} \exp\left(-\frac{3v^2}{2\tilde{A}}\right), \quad (30)$$

we find that $\tilde{A}_0^{1/2} = 1831 \text{ km/s}$ for $\tilde{A}_c^{1/2} \leq 200 \text{ km/s}$, and $\tilde{A}_0^{1/2} = 2183 \text{ km/s}$ for $\tilde{A}_c^{1/2} = v = 627 \text{ km/s}$. Since $\tilde{A}_0^{1/2}$ changes by less than 20% for the significant cut-off of $\tilde{A}_c^{1/2} = v$, we can take $\tilde{A}_c^{1/2} = 0$.

Using Eq.(10) and $\tilde{A}_0^{1/2} = 1831 \text{ km/s}$, we find

$$\frac{\Omega_0^{1.20}}{2\pi^2} \int_0^\infty \frac{dk}{h \text{ Mpc}^{-1}} \frac{P(k)}{h^{-3} \text{ Mpc}^3} \leq \left(\frac{1831 \text{ km/s}}{100 \text{ km/s}} \right)^2 = 335.3 \quad (31)$$

at 95% CL.

Using Eqs.(7), (8), and (9), we obtain at 95% CL

$$\langle \delta_H^2(R) \rangle < \left(\frac{10.5 h^{-1} \text{ Mpc}}{R} \right)^2,$$

$$\begin{aligned}\left\langle \left(\frac{\delta\rho}{\rho} \right)_R^2 \right\rangle &< \Omega_0^{-1.20} \left(\frac{24.0 \, h^{-1}\text{Mpc}}{R} \right)^2, \\ \left\langle \delta_\Omega^2(R) \right\rangle &< \Omega_0^{-1.20} \left(\frac{43.9 \, h^{-1}\text{Mpc}}{R} \right)^2.\end{aligned}\tag{32}$$

We have used $[x\mathcal{L}(x)]^2 \leq 0.3282$, $x^2(3j_1(x)/x)^2 \leq 1.7123$, and $x^2[3j_1(x)/x - 2\mathcal{L}(x)]^2 \leq 5.7579$.

This calculation provides us with the most robust results, both in the sense of being model independent and of relying only on the largest and most observationally secure CMB anisotropy (the dipole). They are thus also the weakest quantitatively. For example, 10% variations in the expansion rate are allowed on scales of 20,000 km/s ($200 \, h^{-1}\text{Mpc}$) in diameter at 95 percent confidence.

6. Summary

Cosmologists attempt to derive properties of the large-scale structure of space-time from local observations. These extrapolations rely on the assumption that we are probing a fair sample of the universe, so that physical quantities measured locally such as the Hubble’s constant, or the mass-to-light ratio are representative of the universe as a whole.

Large-scale structure generates deviations from the Hubble flow; thus, it is important that measurements of the Hubble’s constant probe a large enough volume so that the effects of peculiar motions are small (Turner, Ostriker, & Cen 1992). In this paper, we have estimated the expected variance in the Hubble’s constant due to large scale structure. We began by considering currently fashionable models, which are consistent with galaxy surveys on small scales and CMB observations on large scales. In these models, measurements of the Hubble’s constant that are based on galaxies in a sphere of diameter $200 \, h^{-1}\text{Mpc}$ are likely to be within 3 – 6% (95% confidence interval) of the global value, and of order 1 – 2%

in a sphere of $400 h^{-1}\text{Mpc}$ diameter. These limits assume that the current set of large-scale structure models are good approximation to the primordial power spectrum.

The CMB dipole velocity (the velocity of the Galaxy with respect to the CMB rest frame) places a strong constraint on the amplitude of large scale structure. If there were enormous local void and density fluctuations, as suggested by several authors (Harrison 1993, Wu et al. 1995, Wu et al. 1996), then we would expect that the Galaxy would be moving with respect to the microwave background rest frame at a velocity much larger than the measured value of $627 \pm 22 \text{ km/s}$ (Kogut et al. 1993, Fixsen et al. 1994). Thus, the measured CMB dipole velocity can be used to derive strong constraints on density fluctuations on scales larger than those probed by redshift surveys. We have used these constraints to calculate the variations in the Hubble’s constant, δ_H , for power spectra which have a sharp bump on unobserved scales; we find that the 95% CL upper limit of $|\delta_H|$ increases approximately by a factor of two.

Finally, we have used the constraints derived from the CMB dipole velocity to place a robust limit on variations in the Hubble’s constant. With the CMB dipole measurement alone, we are able to constrain variations in the Hubble’s constant to be less than 10% on scales of $20,000 \text{ km/s}$ ($200 h^{-1}\text{Mpc}$) in diameter at 95 percent confidence. Thus, measurements of H_0 that probe out to this scale are likely to be accurately probing the global expansion rate of the universe.

7. Acknowledgements

Y.W. and E.L.T. acknowledge support from NSF grant AST94-19400. DNS acknowledges support from the MAP/MIDEX project.

REFERENCES

- Bardeen, J.M., Bond, J.R., Kaiser, N., & Szalay, A.S. 1986, ApJ, 304, 15.
- Bennett, C.L., Banday, A.J., Gorski, K.M, Hinshaw, G., Jackson, P., Keegstra, P., Kogut, A., Smoot, G.F., Wilkinson, D.T., & Wright, E.L. 1996, ApJ, 464, L1.
- Birkinshaw, M., Hughes, J.P. & Arnaud, K.A. 1991, ApJ, 379, 466.
- Broadhurst, T., Ellis, R.S., Koo, D.Z., & Szalay, A.S., 1990, Nature, 343, 726.
- Bunn, E.F. & White, M. 1997, ApJ, 480, 6.
- Cohen, J.G., Hogg, D.W., Pahre, M.A., & Blandford, R. 1996, ApJ, 462, L9.
- Da Costa, L.N., Vogeley, M.S., Geller, M.J., Huchra, J.P. & Park, C. 1994, ApJ, 437, L1 - L4.
- Eastman, R.G., Schmidt, B.P., & Kirshner, R.P. 1996, ApJ, 466, 911.
- Fixsen, D.J., Cheng, E.S., Cottingham, D.A., Eplee, R.E., Jr., Isaacman, R.B., Mather, J.C., Meyer, S.S., Noerdlinger, P.D., Shafer, R.A., Weiss, R., Wright, E.L., Bennett, C.L., Boggess, N.W., Kelsall, T., Moseley, S.H., Silverberg, R.F., Smoot, G.F., & Wilkinson, D.T. 1994, ApJ, 420, 445.
- Graham, J.A. et al. 1997, ApJ, 477, 535.
- Harrison, E. 1993, ApJ, 405, L1.
- Hu, W. & Sugiyama, N. 1996, ApJ, 471, 542.
- Jones, M., Saunders, R., Alexander, P., Birkinshaw, M., Grainge, K., Hancock, S., Lasenby, A., Lefebvre, D. & Pooley, G. 1993, Nature, 365, 320.

- Kogut, A., Lineweaver, C., Smoot, G.F., Bennett, C.L., Banday, A., Boggess, N.W, Cheng, E.S., de Amici, G., Fixsen, D.J., Hinshaw, G., Jackson, P.D., Janssen, M., Keegstra, P., Loewenstein, K., Lubin, P., Mather, J.C, Tenorio, L., Weiss, R., Wilkinson, D.T. & Wright, E.L. 1993, ApJ, 419, 1.
- Kundic, T. et al. 1997, ApJ, 482, 75.
- Landy, S.D., Shechtman, S.A., Lin, H. Kirshner, R.P., Oemler, A.E., & Tucker, D. 1996, ApJ, 456, L1.
- Lauer, T.R. & Postman, M. 1994, ApJ, 425, L418.
- Lin, H. et. al. 1996, ApJ, 471, 617.
- Nakamura, T., Nakao, K.-I., Chiba, T. & Shiromizu, T. 1995, MNRAS, 276, L41.
- Nakao, K.-I., Gouda, N., Chiba, T., Ikeuchi, S., Nakamura, T. & Shibata, M. 1995, ApJ, 453, 541.
- Netterfield, C.B., Devlin, M.J., Jarosik, N., Page, L., & Wollack, E.J. 1997, ApJ, 474, 47.
- Peebles, P.J.E., (Princeton University Press, 1980), “The Large-Scale Structure of the Universe”.
- Peebles, P.J.E., (Princeton University Press, 1993), “Principles of Physical Cosmology”.
- Phillips, L.A., & Turner, E.L., in preparation.
- Ratra, B., Sugiyama, N., Banday, A. & Gorski, K.M. 1997, ApJ, 481, 22.
- Schechter, P.L. et al. 1997, ApJ, 475, L85.
- Shi, X. & Turner, M.S. 1997, astro-ph/9707101.
- Shi, X., Widrow, L.M., & Dursi, L.J. 1996, MNRAS, 281, 565.

- Songaila, A., Wampler, E.J. & Cowie, L.L. 1997, *Nature*, 385, 137.
- Strauss, M.A. & Willick, J.A. 1995, *Phys. Reports*, 261, 271 - 431.
- Strauss, M.A., Cen, R., Ostriker, J.P., Lauer, T.R. & Postman, M. 1995, *ApJ*, 444, 507.
- Tadros, H. & Efstathiou, G. 1996, *MNRAS*, 282, 1381.
- Tonry, J.L., Blakslee, J.P., Ajhar, E. & Dressler, A. 1997, *ApJ*, 475, 399.
- Turner, E.L., Ostriker, J.P., & Cen, R. 1992, *AJ*, 103, 1427.
- Wu, X.-P., Deng, Z., Zou, Z., Fang, L.-Z., Qin, B. 1995, *ApJ*, 448, L65.
- Wu, X.-P., Qin, B. & Fang, L.-Z. 1996, *ApJ*, 469, 48.

Fig. 1.— Window functions of $\langle \delta_H^2 \rangle_R$ (solid line), $\langle (\delta\rho/\rho)^2 \rangle_R$ (dotted line), $\langle \delta_\Omega^2 \rangle_R$ (short-dashed line), and $\langle \mathbf{v}^2 \rangle_R$ (long-dashed line).

Fig. 2.— $\langle \delta_H^2 \rangle_R$ as function of R , for the three models (TCDM, Λ CDM, and OCDM).

Fig. 3.— $\langle (\delta\rho/\rho)^2 \rangle_R$ as function of R , for the three models (TCDM, Λ CDM, and OCDM).

Fig. 4.— $\langle \delta_\Omega^2 \rangle_R$ as function of R , for the three models (TCDM, Λ CDM, and OCDM).

Fig. 5.— $\langle \mathbf{v}^2 \rangle_R$ as function of R , for the three models (TCDM, Λ CDM, and OCDM).

Fig. 6.— $P(\delta_H|v)_R$ for $k_0 = 0.01 h\text{Mpc}^{-1}$ and $R = 40 h^{-1}\text{Mpc}$. The solid and dashed lines are the distributions given by Eq.(23), with $x_c = 10$ ($A_c = 0.1 \alpha_1/\alpha_2$) and $x_c = 1$ ($A_c = \alpha_1/\alpha_2$) respectively; the dotted lines are Gaussian distributions with the same variance [given by Eq.(26)] for $x_c = 10$.

Fig. 7.— Same as Fig.6, for $R = 100 h^{-1}\text{Mpc}$.

Fig. 8.— Same as Fig.6, for $R = 500 h^{-1}\text{Mpc}$.

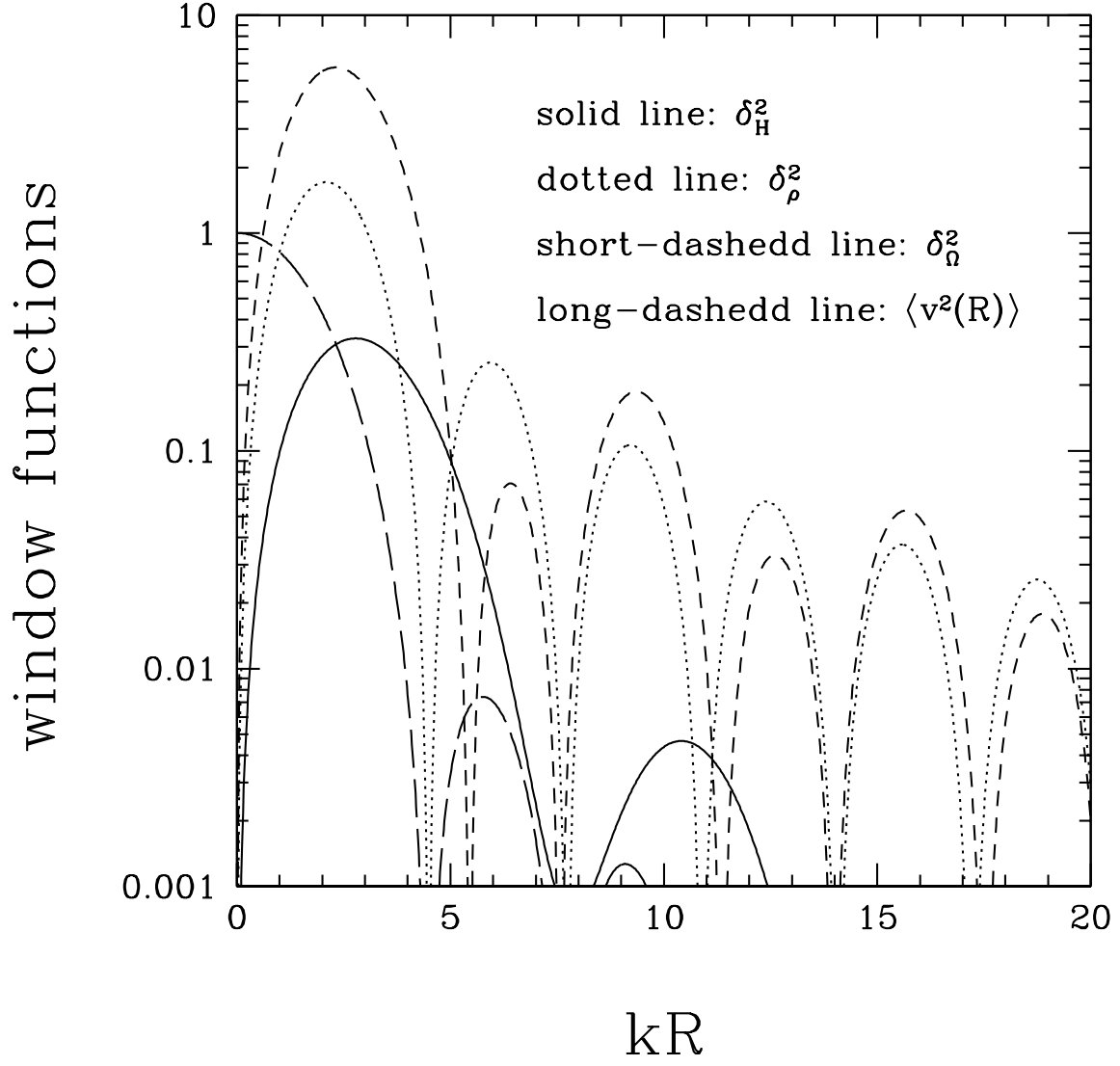


Fig. 1.— Window functions of $\langle \delta_H^2 \rangle_R$ (solid line), $\langle (\delta\rho/\rho)^2 \rangle_R$ (dotted line), $\langle \delta_\Omega^2 \rangle_R$ (short-dashed line), and $\langle \mathbf{v}^2 \rangle_R$ (long-dashed line).

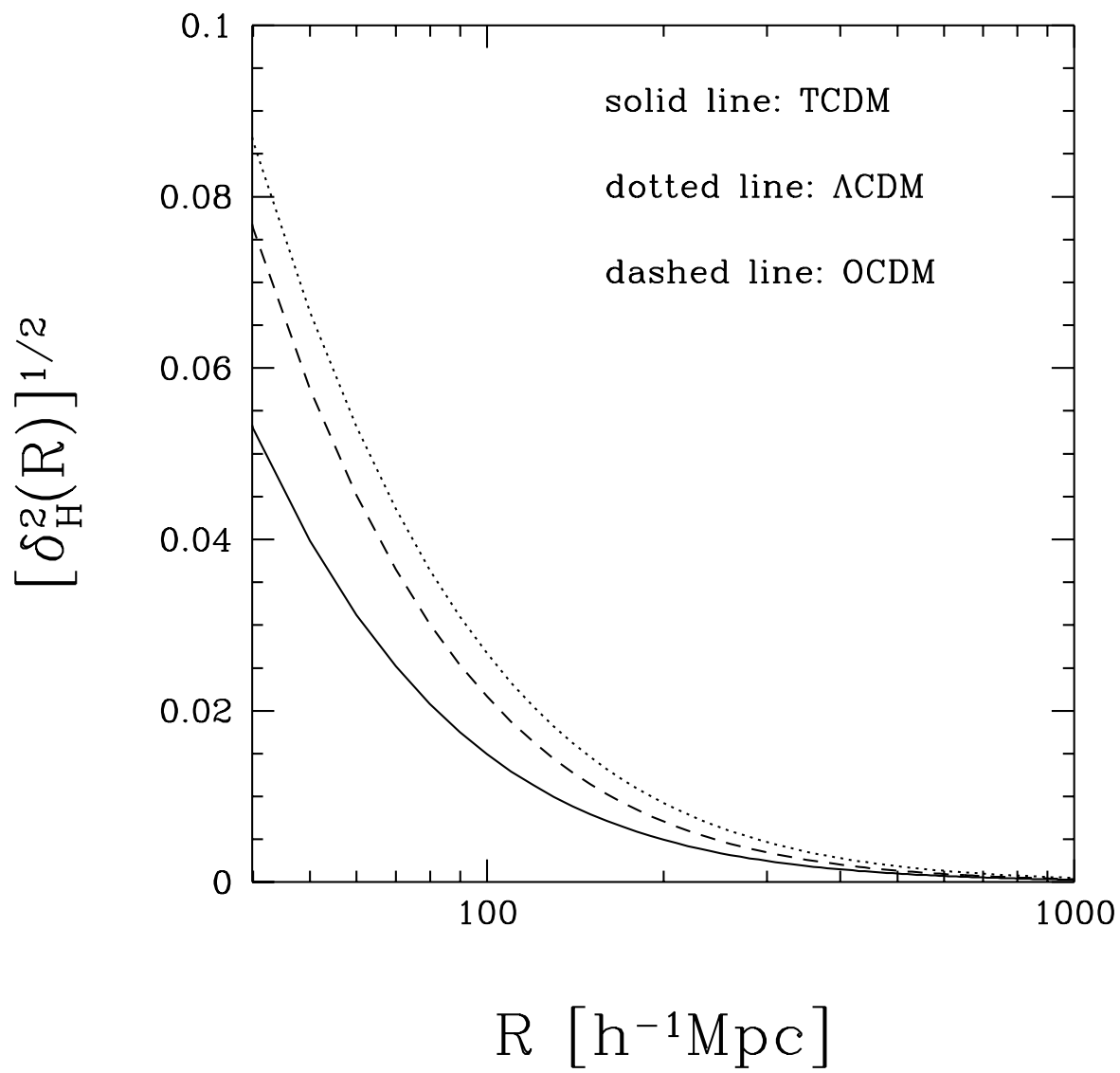


Fig. 2.— $\langle \delta_H^2 \rangle_R$ as function of R , for the three models (TCDM, Λ CDM, and OCDM).

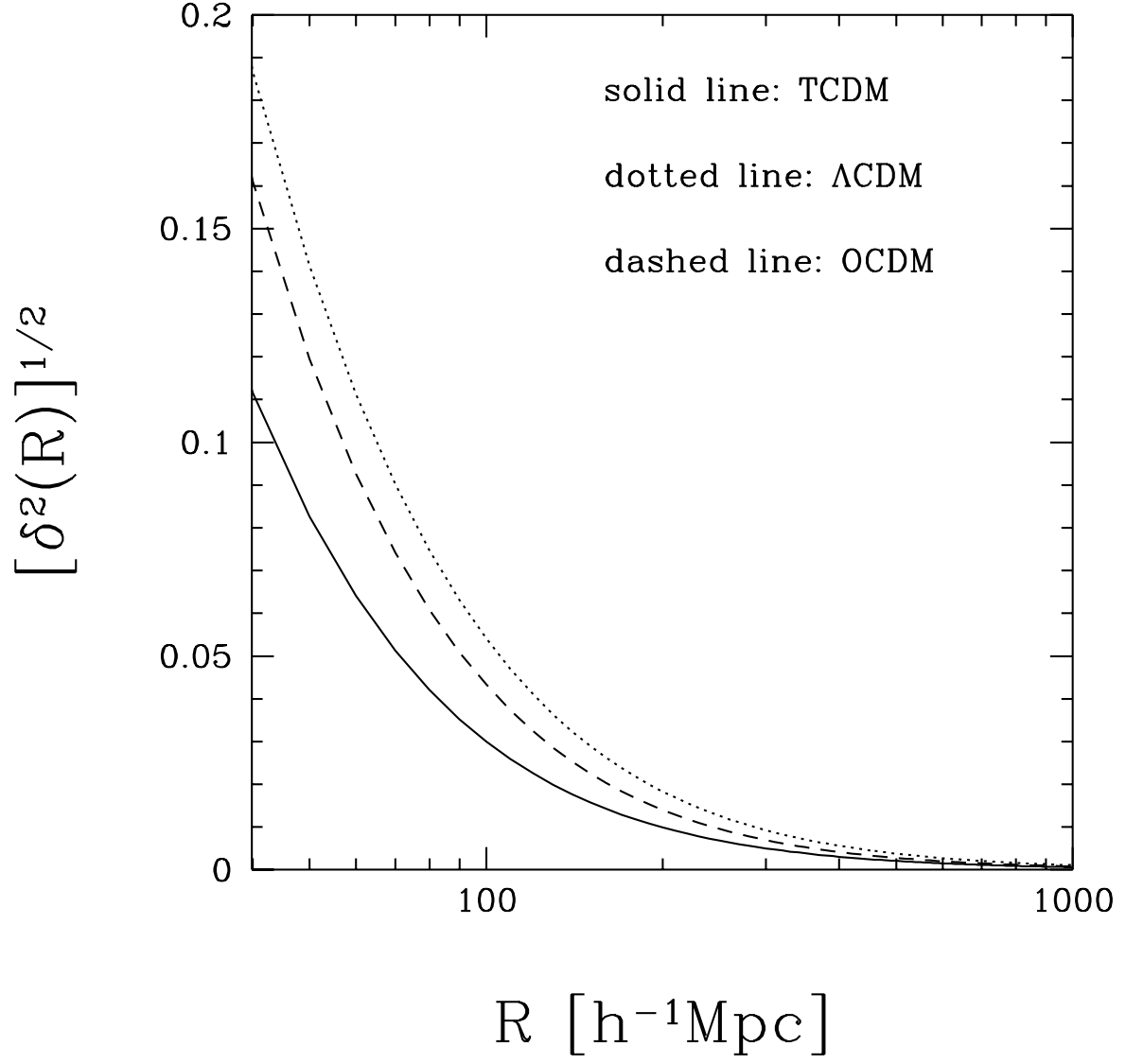


Fig. 3.— $\langle(\delta\rho/\rho)^2\rangle_R$ as function of R , for the three models (TCDM, Λ CDM, and OCDM).

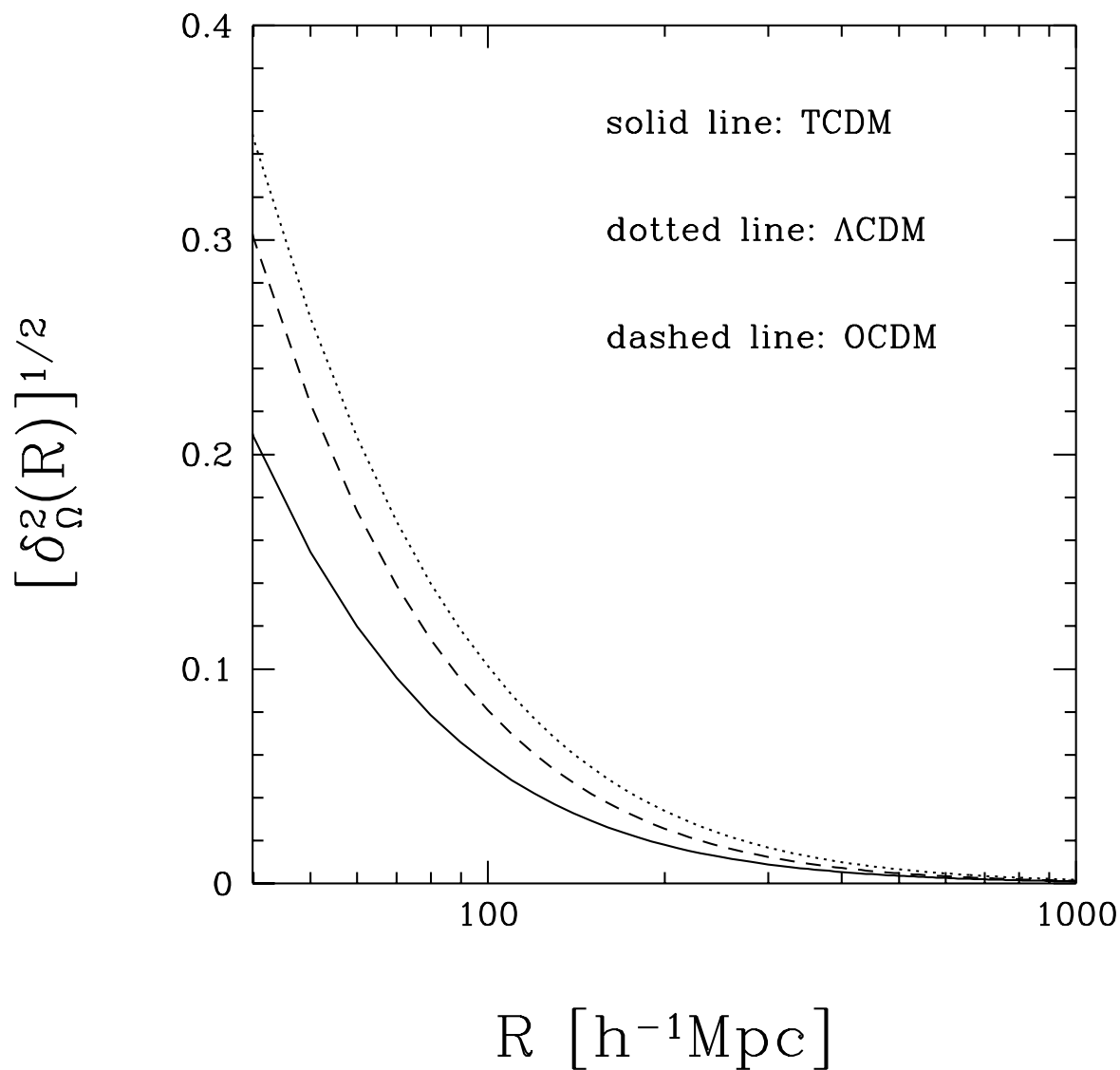


Fig. 4.— $\langle \delta_{\Omega}^2 \rangle_R$ as function of R , for the three models (TCDM, Λ CDM, and OCDM).

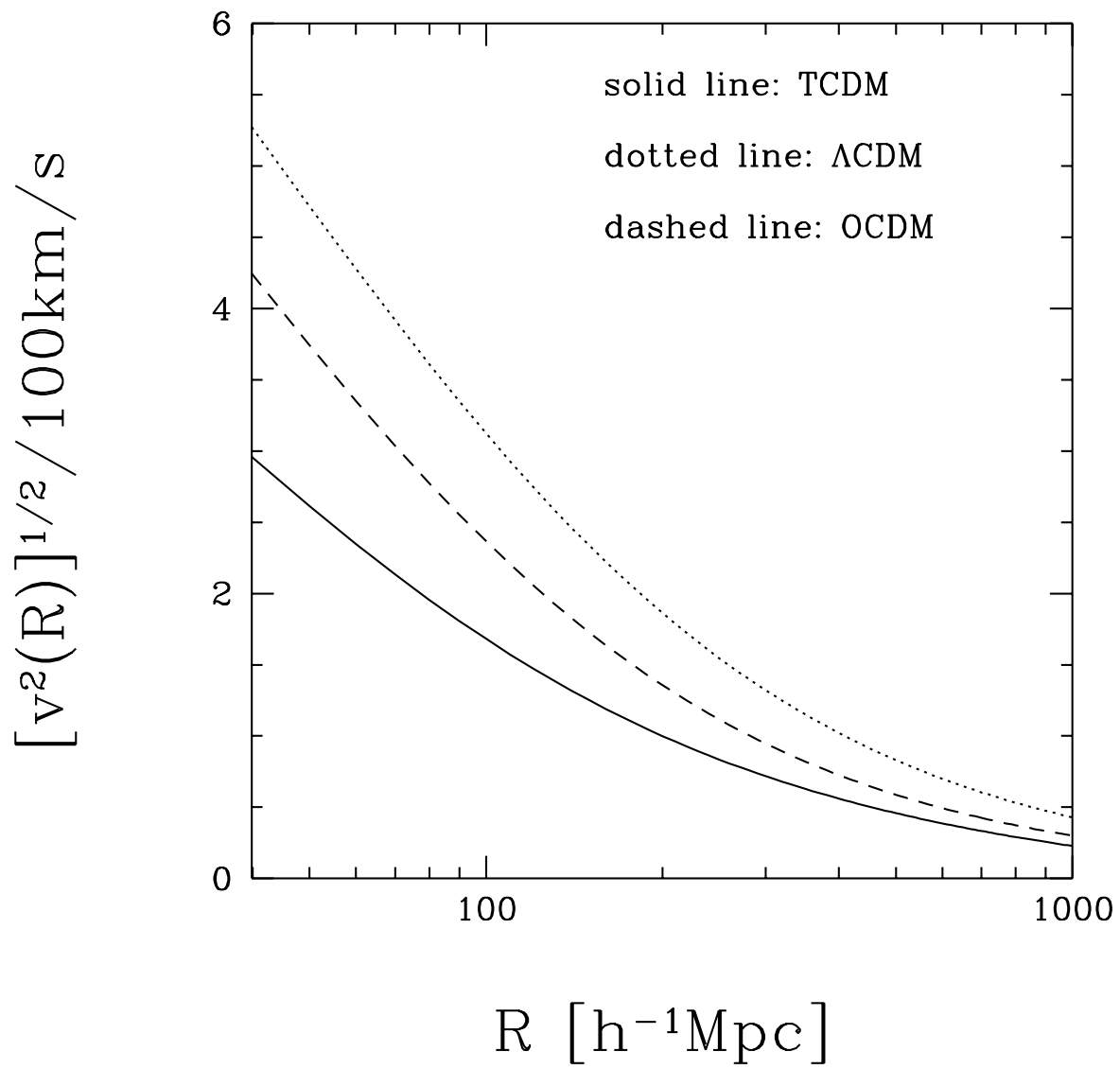


Fig. 5.— $\langle \mathbf{v}^2 \rangle_R$ as function of R , for the three models (TCDM, Λ CDM, and OCDM).

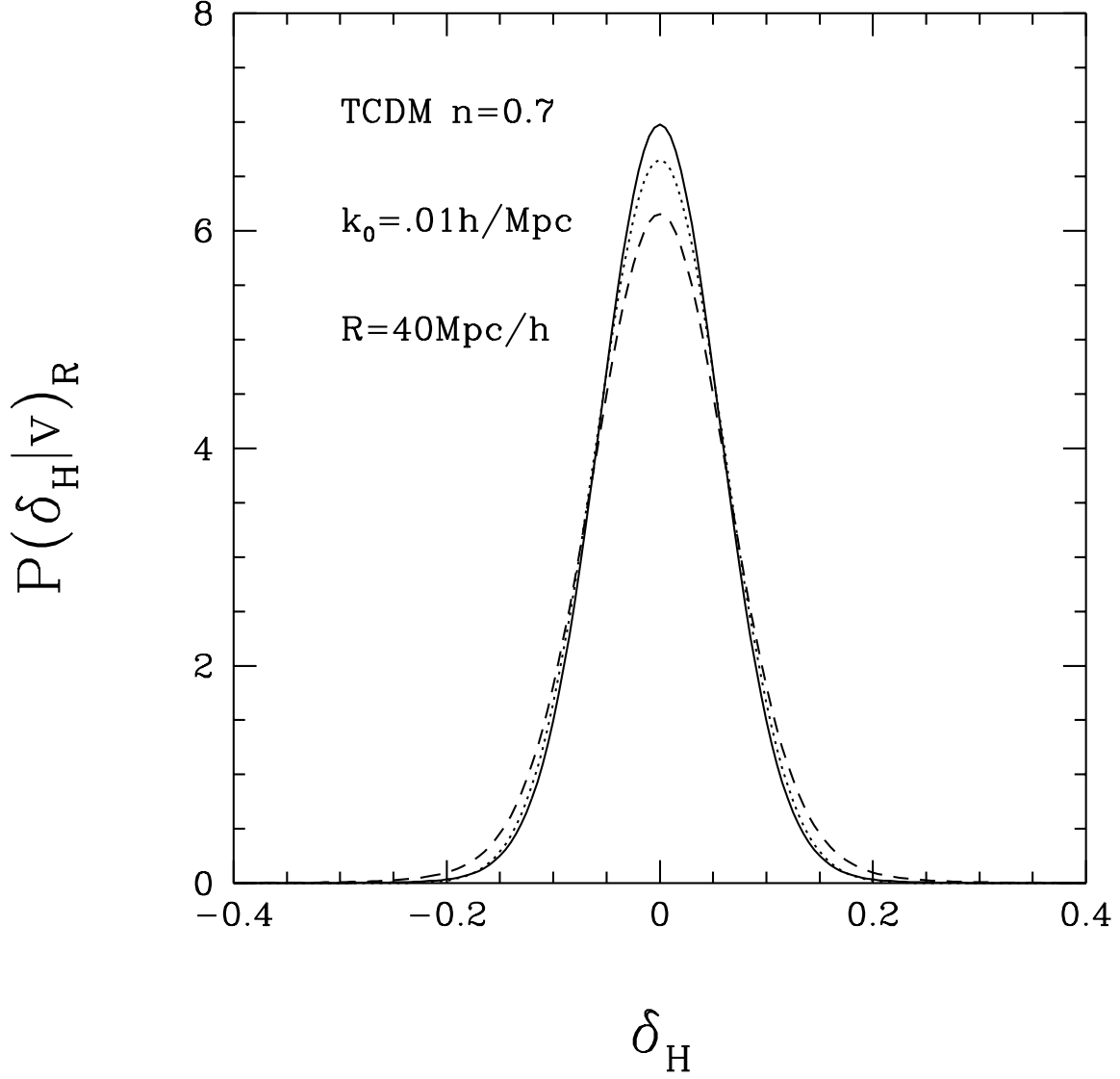


Fig. 6.— $P(\delta_H|v)_R$ for $k_0 = 0.01 h\text{Mpc}^{-1}$ and $R = 40 h^{-1}\text{Mpc}$. The solid and dashed lines are the distributions given by Eq.(23), with $x_c = 10$ ($A_c = 0.1 \alpha_1/\alpha_2$) and $x_c = 1$ ($A_c = \alpha_1/\alpha_2$) respectively; the dotted lines are Gaussian distributions with the same variance [given by Eq.(26)] for $x_c = 10$.

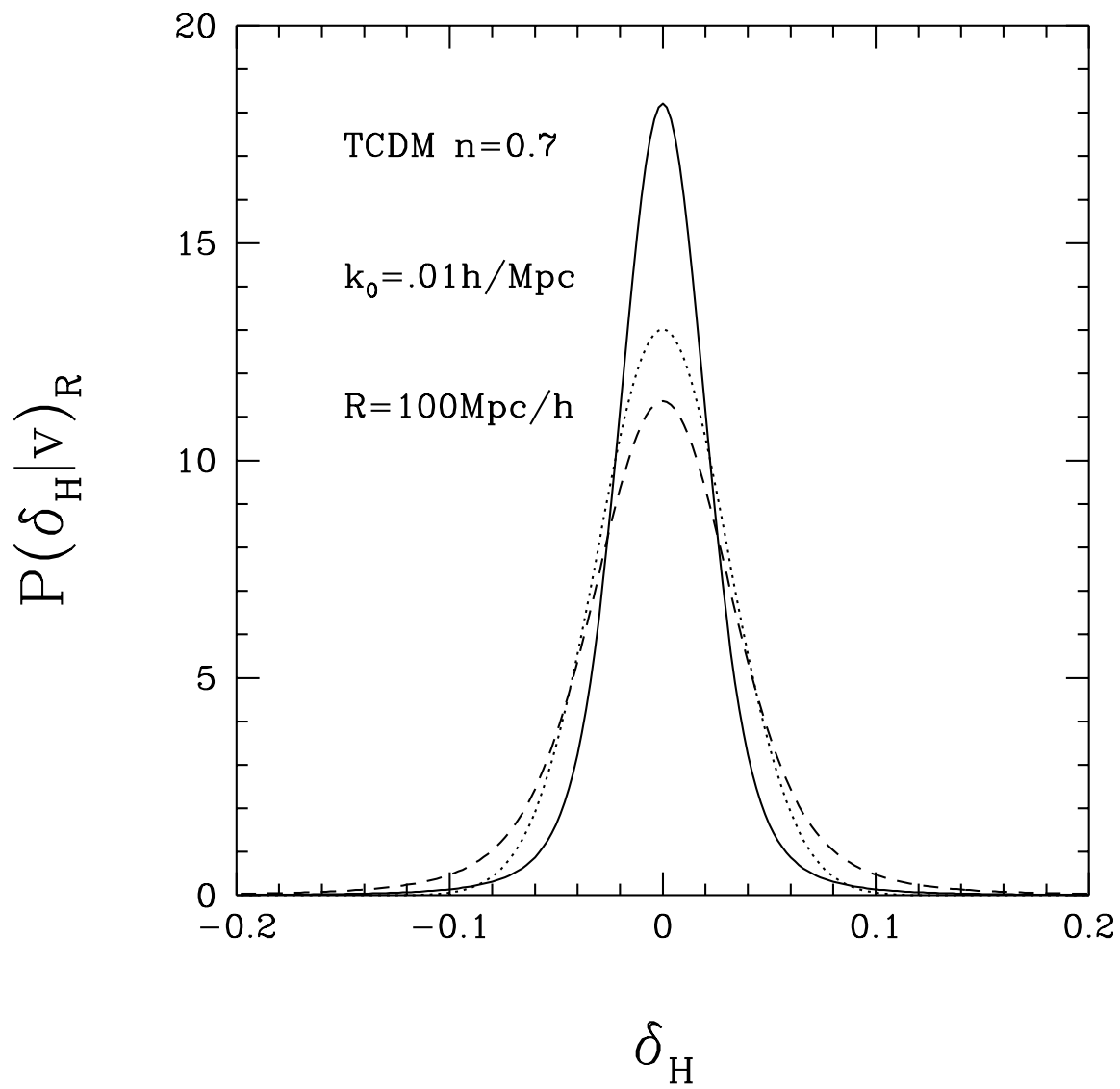


Fig. 7.— Same as Fig.6, for $R = 100 h^{-1} \text{Mpc}$.

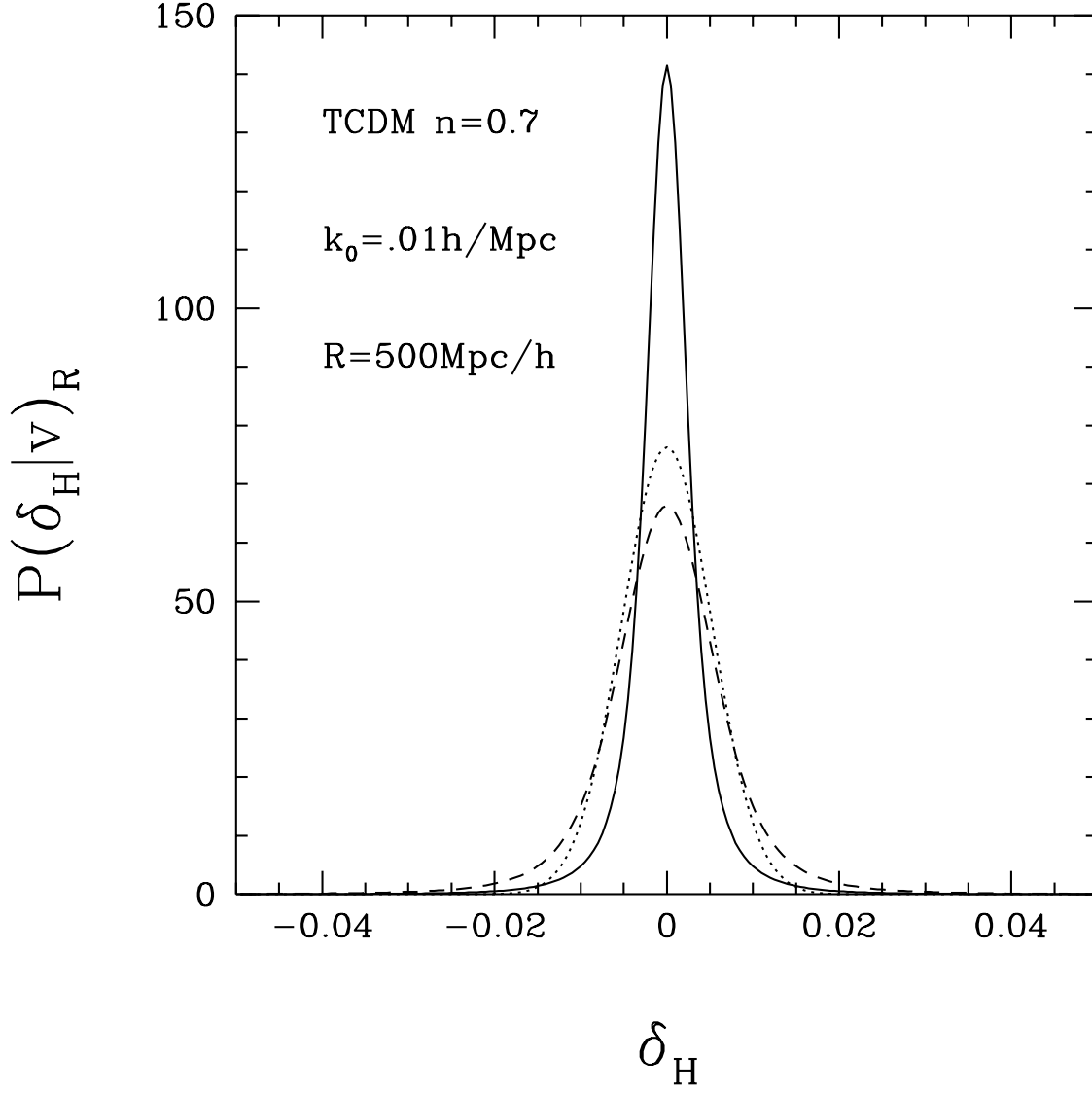


Fig. 8.— Same as Fig.6, for $R = 500 h^{-1} \text{Mpc}$.